Supporting Information

Solvent bath annealing-induced liquid phase Ostwald ripening enabling efficient and stable perovskite solar cells

*Rui Meng[1, †], Can Li[1, †], Lei Yang[1], Zhihao Li[1], Zhi Wan[1], Jishan Shi[1], Zhen Li[1, *]*

1. State Key Laboratory of Solidification Processing, Center for Nano Energy Materials, School of Materials Science and Engineering, Northwestern Polytechnical University and Shaanxi Joint Laboratory of Graphene (NPU), Xi'an, 710072, P. R. China

Experimental Section

Materials: Cesium iodide (CsI, 99.99%), Spiro-OMeTAD (99.9%), tris(2-(1H-pyrazol-1-yl)-4-tert-butylpyridine)-cobalt(III)tris(bis(trifluoromethylsulfonyl)imide) (FK209, 99%), bis(trifluoromethanesulfonyl)imide (Li-TFSI, 99%) and 4-tert-butyl pyridine (tBP, 96%) were purchased from Xi'an Polymer Light Technology Corp. Tin (IV) chloride pentahydrate ($SnCl_4 \cdot 5H_2O$) were purchased from Aladdin. Formamidine iodide (FAI, 99.9%) and methylammonium bromine (MABr, 99.9%) were purchased from Great cell. Lead bromide ($PbBr_2$, 99.9%) and lead iodide (PbI_2, 99.9%) were purchased from TCI. Dimethylformamide (DMF, >99.9%), dimethyl sulfoxide (DMSO, 99.9%), chlorobenzene (CB, 99.9%) and acetonitrile were purchased from Sigma-Aldrich. 1H, 1H-perfluorooctylamine (PFA, 99.9%) was purchased from Alfa Aesar. All the reagents were used as received without any further purification.

Precursor solution preparation: The SnO_2 precursor solution (0.2 M) was prepared by dissolving 3.5 g $SnCl_4 \cdot 5H_2O$ in 50 mL ethanol and stirring at 90 ℃ for 7 h. For the $Cs_{0.05}(FA_{0.85}MA_{0.15})_{0.95}Pb(I_{0.85}Br_{0.15})_3$ precursor solution, CsI (0.07 M), FAI (1.19 M), MABr (0.21 M), $PbBr_2$ (0.21 M) and PbI_2 (1.3 M) were dissolved in a mixed solvent (DMF: DMSO = 4:1). The hole transport layer (HTL) solution was prepared by dissolving 80 mg spiro-OMeTAD, 36 μL tBP, 20 μL Li-TFSI (520 mg/mL in acetonitrile) and 16 μL FK209 (300 mg/mL in acetonitrile) in 1 mL CB.

Device fabrication: The ITO substrate was cleaned by deionized water, acetone, and ethanol successively. After 15 min UV-ozone treatment, 70 μL SnO_2 precursor solution was spin-coated on the substrate at 6000 rpm for 30 s, followed by annealing

at 175 °C for 30 min to prepare the electron transport layer (ETL). After 15 min UV-Ozone treatment, the substrate was transferred to a nitrogen-filled glove box. The perovskite precursor solution was spun onto the substrate at 1000 rpm for 10 s and 6000 rpm for 30 s, and 120 μL of CB was dropped at 15th second of spinning. For TA process, the perovskite film was thermally annealed at 100 °C for 60 min. For SVA process, about 10 μL of DMF was dropped around the film during thermal annealing, covered by a petri dish to create a DMF vapor atmosphere, and then thermally annealed at 100 °C for 60 min. For SBA process, the perovskite film was immersed in a mixed solvent of CB and DMF (100:x, x=0-4, v/v) and annealed at 100 °C for 60 min. For PFA-SBA, different volume concentrations of PFA were further added in a mixed solvent of CB and DMF (100:1, v/v), followed by annealing at 100 °C for 60 min. For SBA and PFA-SBA, the perovskite films were thermally annealed at 100 °C for 2 min after liquid phase annealing to remove excess solvent. The HTL precursor solution was spun onto the perovskite film at 5000 rpm for 30 s. Finally, 100 nm Au electrodes were thermally evaporated in vacuum.

Thin film and device characterization: The morphologies of the perovskite films were measured by field-emission scanning electron microscopy (SEM) (FEI NAVA 450). XRD patterns were measured by X-ray diffractometer (Bruker D8 Discover A25). The UV-vis absorption spectra of the samples were obtained by UV-vis spectrophotometer (Lambda 35). PL spectra were collected using an Ocean Optics QE Pro spectrometer with an excitation wavelength of 532 nm. TRPL spectra were collected using a Horiba PPD 900 spectrometer with an excitation wavelength of 770

nm. XPS measurements were performed using a Shimadzu Kratos photoelectron spectrometer. FTIR spectra were recorded with a Thermo Nicolet 6700 spectrometer. The surface structure and roughness of the samples were characterized by atomic force microscopy (AFM, Bruker Dimension Icon). The *J-V* characteristics of PSCs were recorded by a Keithley 2400 source-measurement unit with a solar simulator (Newport, Sol3A) under AM1.5G (100 mW/cm^2) illumination. The light intensity was calibrated through standard silicon solar cells. The scan speed was 0.1 V/s (-0.1 V-1.2 V). The incident photoelectron conversion efficiency (IPCE) was measured by a quantum efficiency measurement system (Enli Tech, QE-R3011).

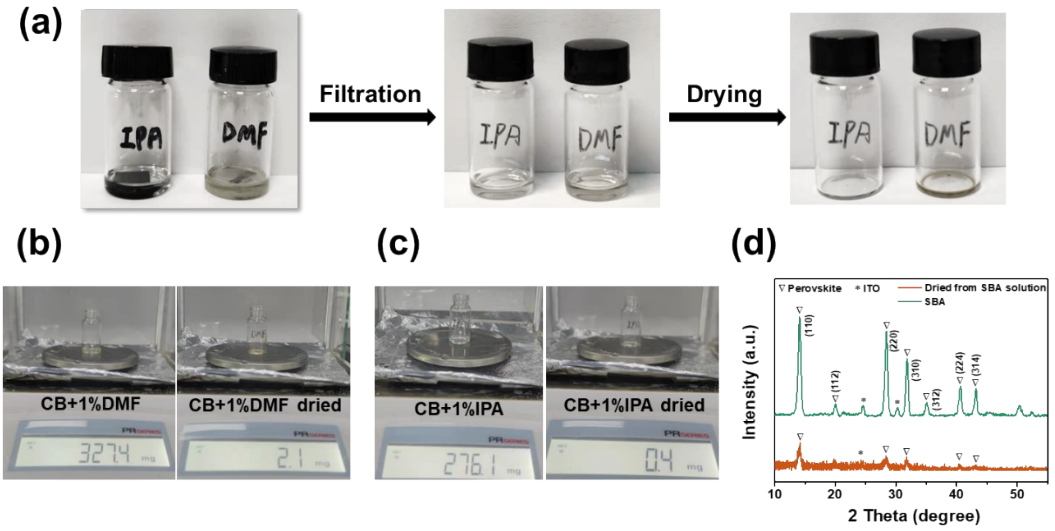

Figure S1. (a) Images of the residual solvents of SBA with IPA and DMF as polar solvents after filtering and drying, respectively. Images of the weight of residual solvent in SBA based on (b) DMF, (c) IPA after filtration and drying, respectively. (d) XRD spectra of the perovskite film with SBA treatment and the residual powder dried from the solvents after SBA treatment.

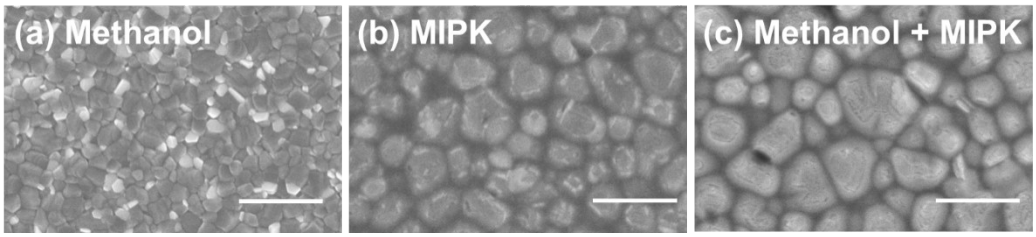

Figure S2. SEM images of perovskite films based on SBA treatment with different polar solvents: (a) Methanol, (b) MIPK, (c) Methanol and MIPK. (Scale bar: 1μm).

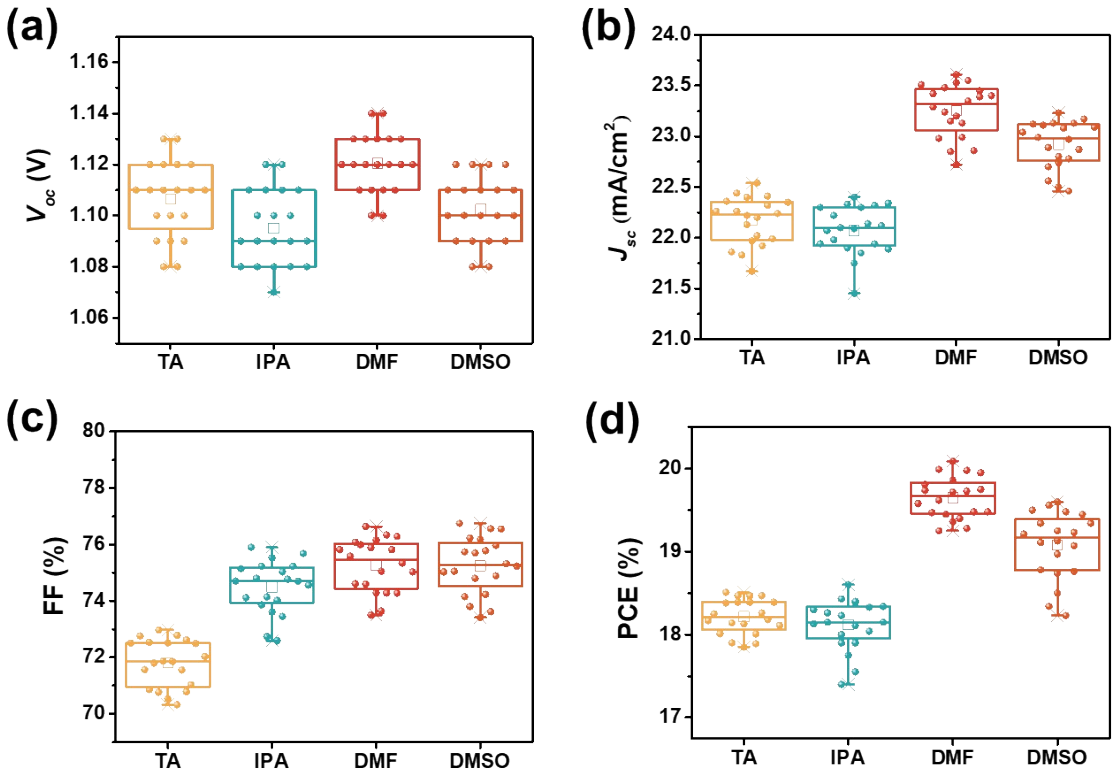

Figure S3. Photovoltaic parameters statistics of PSCs based on TA and SBA treatment with different polar solvent: (a) V_{oc}, (b) J_{sc}, (c) FF and (d) PCE.

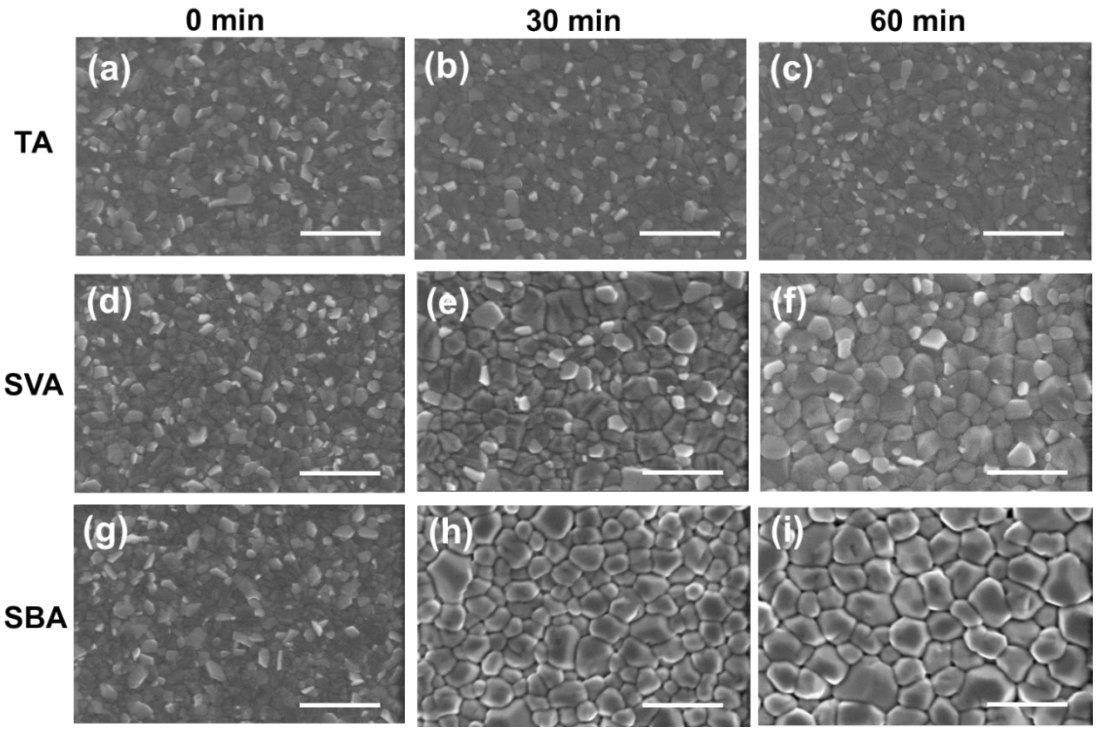

Figure S4. SEM images of perovskite films based on different treatments and annealing time: (a) TA-0 min, (b) TA-30 min, (c) TA-60 min, (d) SVA-0 min, (e) SVA-30 min, (f) SVA-60 min, (g) SBA-0 min, (h) SBA-30 min, (i) SBA-60 min. (Scale bar: 1 μm)

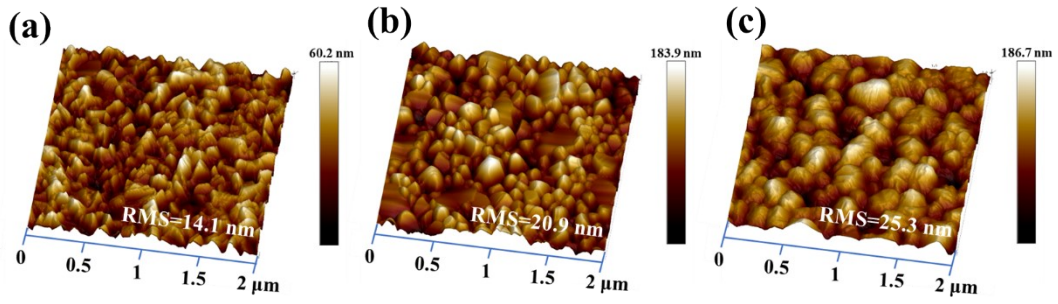

Figure S5. AFM images of perovskite films based on (a) TA; (b) SVA and (c) SBA.

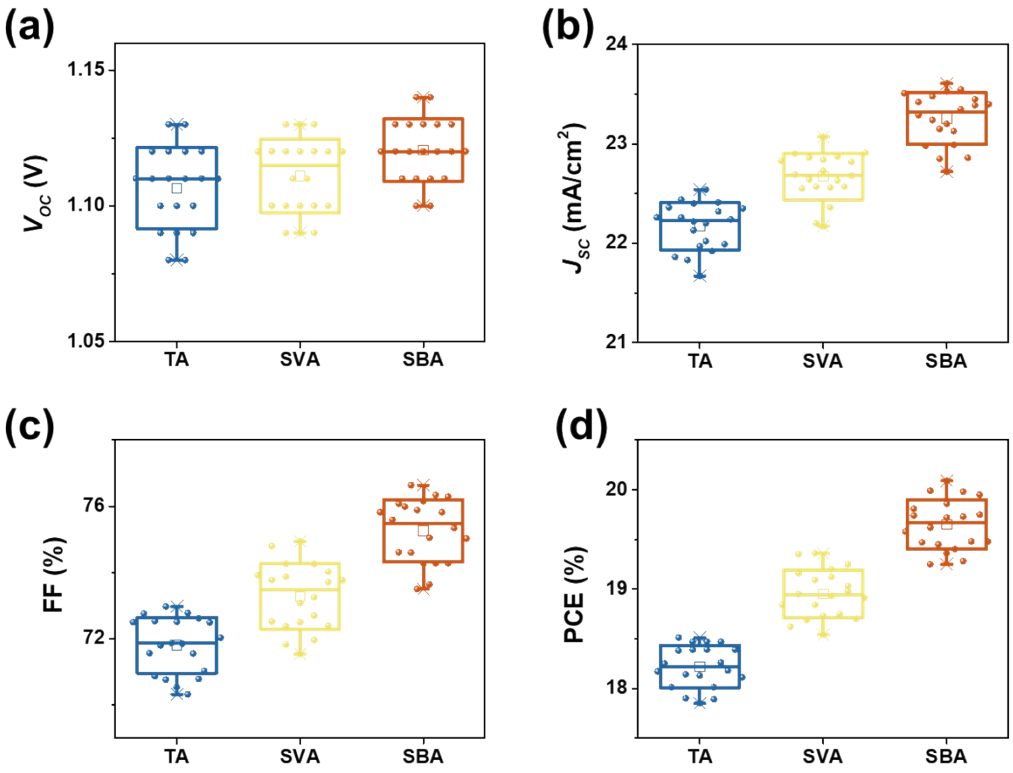

Figure S6. Photovoltaic parameters statistics of PSCs with different treatments.

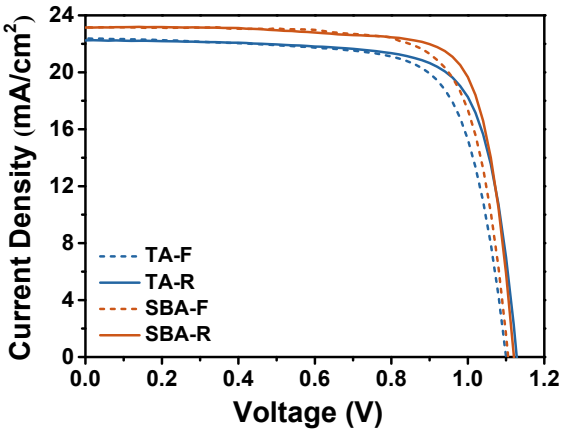

Figure S7. *J-V* curves measured under reverse and forward scans based on TA and SBA treatments.

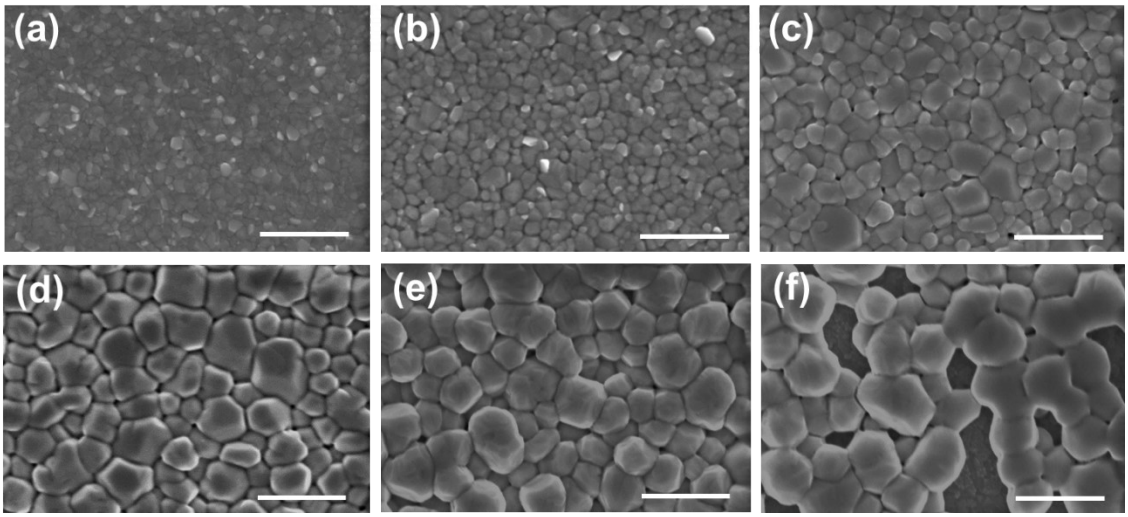

Figure S8. SEM images of perovskite films based on TA and SBA treatments with different DMF concentrations: (a) TA; (b) SBA (0% DMF); (c) SBA (0.5% DMF); (d) SBA (1% DMF); (e) SBA (2% DMF); (f) SBA (4% DMF). (Scale bar: 1 μm)

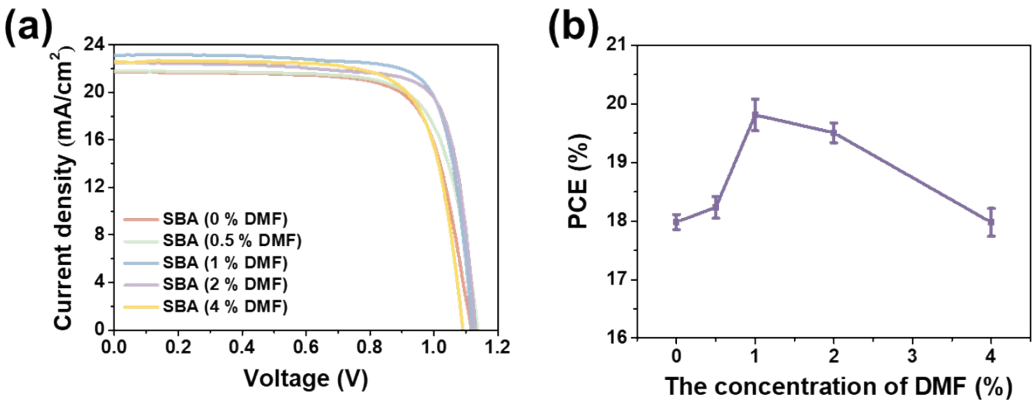

Figure S9. (a) *J-V* curves of PSCs based on SBA treatments with different DMF concentrations. (b) The relationship between PCE of PSCs and DMF concentration in mixed solvent during SBA treatment.

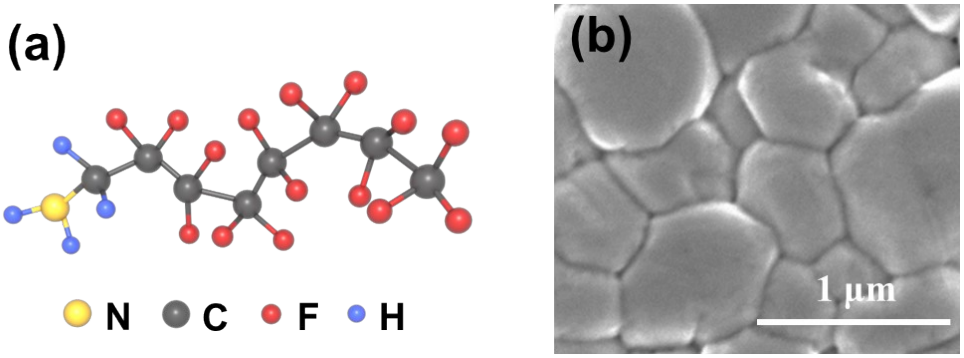

Figure S10. (a) Schematic diagram of the molecular structure of 1H, 1H-perfluorooctylamine (PFA). (b) SEM images of perovskite films based on PFA-SBA treatments.

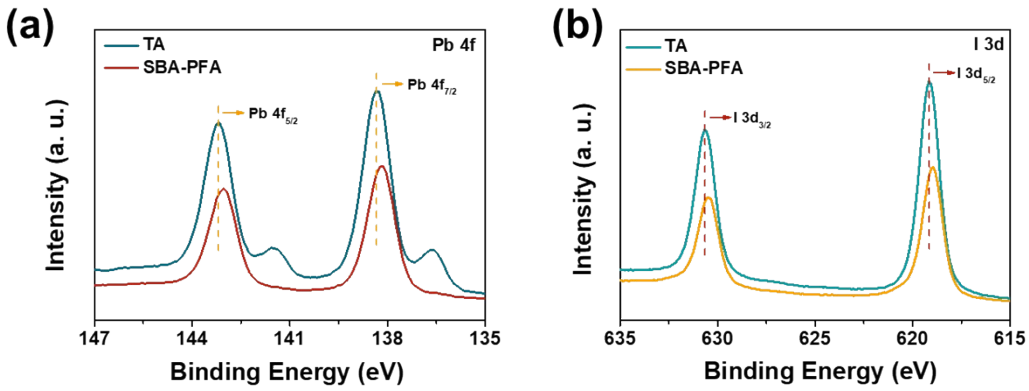

Figure S11. X-ray photoelectron spectroscopy (XPS) of (a) Pb 4f, (b) I 3d of the perovskite film based on TA and SBA-PFA. (Note: To exclude the effect of DMF on perovskite, DMF was not added to the SBA-PFA here.)

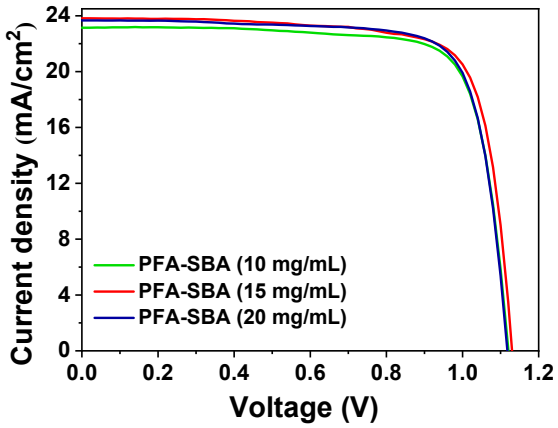

Figure S12. *J-V* curves of PSCs based on PFA-SBA treatments with different PFA concentrations.

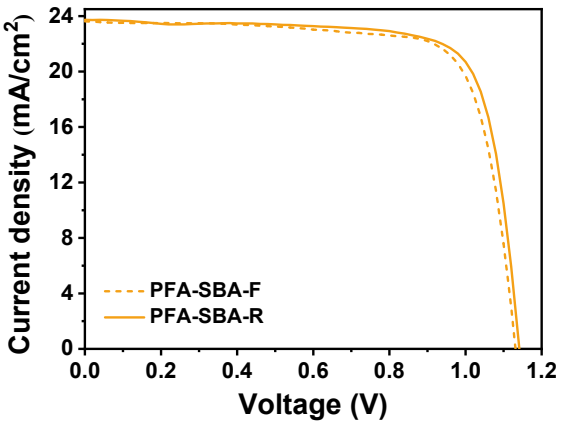

Figure S13. *J-V* curves of PSCs measured under reverse and forward scans based on PFA-SBA treatments.

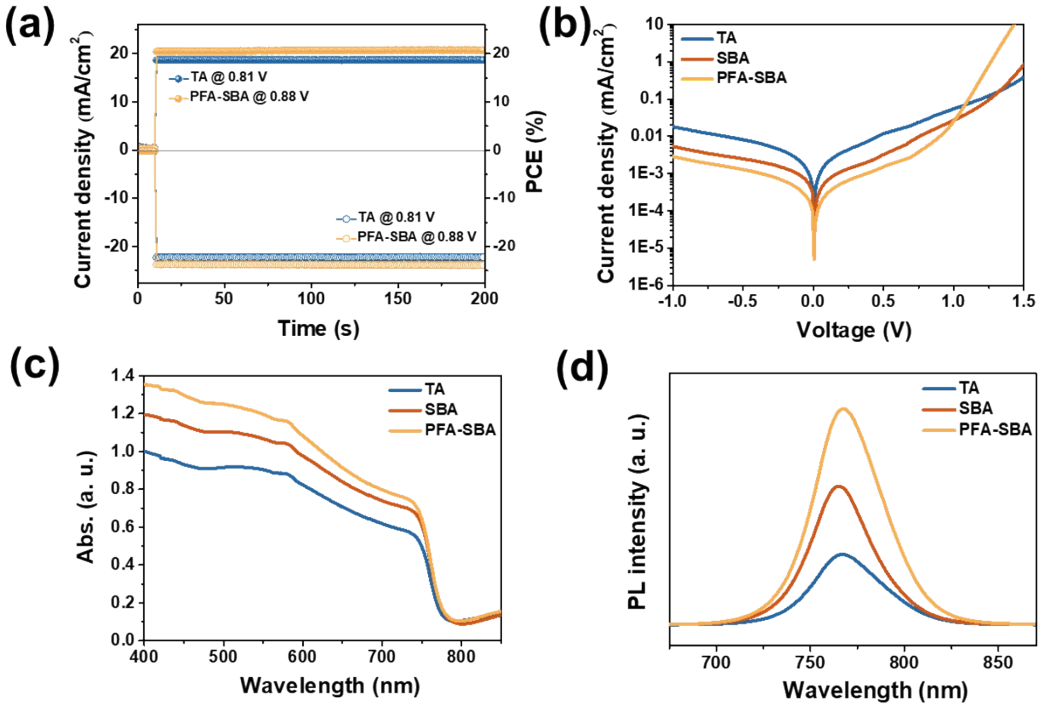

Figure S14. (a) Steady-state output measurements at maximum power point of the TA-PSCs and PFA-SBA-PSCs. (b) dark *J-V* curves, (c) UV-vis absorption spectra, (d) steady-state PL spectra of perovskite films based on TA, SBA and PFA-SBA treatments.

Table S1. The solubility (S) of FAI and PbI_2 in solvents of different polarity at room temperature (20 °C). The solubility was classified into three categories: good (green) with S≥10; medium (yellow) with 0.1≤S<10; poor (red) with S ≤0.1.

Solvent	Polarity	FAI (g/100 g)	PbI_2 (g/100 g)	Grain growth
IPA	**4.3**	**12.74**	**-**	**No**
MIPK	**4.5**	**1.00**	**6.21**	**Moderate**
Acetone	**5.4**	**4.85**	**-**	**No**
Acetonitrile	**6.2**	**7.07**	**-**	**No**
DMF	**6.4**	**87.84**	**31.00**	**Yes**
Methanol	**6.6**	**79.11**	**-**	**No**
DMSO	**7.2**	**65.83**	**34.92**	**Yes**

Table S2. PV parameters of PSCs based on SBA treatments with different DMF concentrations.

	V_{oc} (V)	J_{sc} (mA/cm²)	FF (%)	PCE (%)
0% DMF	1.12±0.01	21.97±0.24	71.8±2.1	17.98±0.13
0.5% DMF	1.12±0.01	22.00±0.28	73.4±1.8	18.23±0.19
1% DMF	1.12±0.01	23.24±0.23	76.0±1.2	19.81±0.27
2% DMF	1.13±0.01	23.06±0.37	74.8±2.1	19.51±0.17
4% DMF	1.10±0.01	22.05±0.37	71.2±2.1	17.97±0.24

Table S3. PV parameters of PSCs based on PFA-SBA treatments with different PFA concentrations.

	V_{oc} (V)	J_{sc} (mA/cm^2)	FF (%)	PCE (%)
PFA-SBA (0 mg/mL)	1.12±0.01	23.62±0.38	76.1±1.9	20.11±0.34
PFA-SBA (5 mg/mL)	1.12±0.01	23.71±0.32	76.8±2.2	20.39±0.32
PFA-SBA (10 mg/mL)	1.13±0.01	23.68±0.37	77.3±1.8	20.51±0.25
PFA-SBA (15 mg/mL)	1.13±0.01	23.73±0.33	78.2±2.0	20.75±0.19
PFA-SBA (20 mg/mL)	1.13±0.01	23.71±0.39	77.1±1.8	20.64±0.21

Table S4. PV parameters of PSCs based on TA, SBA and PFA-SBA treatments.

		V_{oc} (V)	J_{sc} (mA/cm^2)	FF (%)	PCE (%)	Hysteresis index (%)
TA	F	1.09	22.33	70.21	17.08	7.3
	R	1.12	22.42	73.43	18.43	
SBA	F	1.11	23.22	74.34	19.15	5.4
	R	1.12	23.14	78.06	20.25	
PFA-SBA	F	1.13	23.62	76.2	20.35	2.4
	R	1.14	23.73	77.1	20.86	

Table S5. Fitted parameters for TRPL spectra for perovskite films based on TA, SBA and PFA-SBA treatments.

Sample	τ_1 (ns)	τ_2 (ns)	$\tau_{Avg.}$ (ns)
TA	32	391	137
SBA	39	604	396
PFA-SBA	68	574	428

Table S6. Trap density of PSCs based on TA, SBA and PFA-SBA treatments as determined by the space-charge-limited current (SCLC) method.

Sample	n_t (cm^{-3})
TA	6.09×10^{14}
SBA	4.15×10^{14}
PFA-SBA	3.04×10^{14}